JOURNAL OF THERMOPHYSICS AND HEAT TRANSFER
Vol. 22, No. 4, October–December 2008

Electrothermal Behavior of Conductive Polymer Composite Heating Elements Filled with Ceramic Particles

G. Droval,* P. Glouannec,† P. Salagnac,‡ and J. F. Feller§
Université de Bretagne Sud,
56321 Lorient, France

DOI: 10.2514/1.36193

In this study, the influence of ceramic powders on the electrical and thermal behavior of biphasic conductive polymer composites when subjected to electrical potential difference is investigated by means of experimental measurements and modeling. The biphasic materials studied are blends of a thermal conductive polymer phase (syndiotactic polystyrene filled with aluminum oxide or boron nitride) with an electrical conductive polymer phase (high-density polyethylene filled with carbon black) in a cocontinuous structure. The thermophysical characteristics of the biphasic materials were measured as a function of temperature. This thermophysical characterization showed that the thermal conductivity of conductive polymer composites is doubled when filled with a 20% volume of ceramic powder. Ohmic heating experiments were performed on extruded tapes. A two-dimensional finite element model has been developed to determine the thermal and electrical behavior of these devices. The numerical and experimental results correlated well, which shows the relevance of adding aluminum oxide or boron nitride in the biphasic materials studied to enhance thermal conductivity of biphasic conductive polymer composites without modifying the electrical conductivity.

Nomenclature

C_p	=	specific heat capacity, $J \cdot kg^{-1} \cdot K^{-1}$
E	=	electric field, $V \cdot m^{-1}$
e	=	thickness of the tape
I	=	intensity, A
J	=	current density, $A \cdot m^{-2}$
k	=	thermal conductivity, $W \cdot m^{-1} \cdot K^{-1}$
L	=	length of the tape, m
ℓ	=	height of the tape, m
p	=	internal heat source, $W \cdot m^{-2}$
T	=	temperature, °C
T_{air}	=	air temperature, °C
T_c	=	center temperature, °C
T_s	=	surface temperature, °C
t	=	time, s
V	=	voltage, V
x, y, z	=	Cartesian coordinates, m
α	=	thermal diffusivity, $m^2 \cdot s^{-1}$
ρ	=	density, $kg \cdot m^{-3}$
ρ_e	=	electrical resistivity, $\Omega \cdot cm$
σ	=	electrical conductivity, $S \cdot m^{-1}$
ϕ	=	volume fraction, %
φ	=	heat flux density, $W \cdot m^{-2}$

Subscripts

c	=	composite
f	=	filler
m	=	matrix
r	=	radiative
w	=	wall

Received 17 December 2007; revision received 27 February 2008; accepted for publication 5 March 2008.

*Graduate Research Student, Laboratory of Thermal Studies, Energetic and Environment, Centre de Recherche.

†Professor, Laboratory of Thermal Studies, Energetic and Environment, Centre de Recherche.

‡Assistant Professor, Laboratory of Thermal Studies, Energetic and Environment, Centre de Recherche.

§Professor, Laboratory of Polymer Properties at Interfaces and Composites, Centre de Recherche.

Introduction

CONDUCTING polymer composites (CPC) result from blending insulating polymer and electrically conducting fillers [carbon black (CB), metal particles] [1,2]. Their formulation can be adapted to satisfy different characteristics of electrical properties (resistivity, percolation threshold) with temperature [3], pressure [4], or solvent [5] solicitations. This gives CPC a sensitivity toward their environment. These very versatile materials can be used for several applications, such as self-regulated heating [6,7], electromagnetic shielding [8,9], or vapor sensing [5,10].

For basic applications, to get cheap and easy processing CPC it is useful to reduce the percolation threshold, that is, the quantity of filler beyond which the CPC becomes electrically conductive. This target can be achieved by using cocontinuous biphasic polymers (an immiscible blend), in which the fillers are dispersed in only one phase [11].

Despite the numerous advantages brought about by biphasic CPC, for self-regulated heating applications [6], their low thermal conductivity, resulting from the polymer matrix (which is a good thermal insulator), is a major drawback for reaching high power density levels [12]. In fact, the current going across the filled polymer induces power dissipation by the joule effect, which leads to an important thermal gradient within the material and, in the long run, can damage the device due to unacceptable stresses. A solution to this problem is to improve thermal conductivity by adding thermal conductive fillers in the CPC [13]. However, this addition may also have consequences on electrical properties.

The high-density polyethylene (HDPE) is used for its excellent capacity for self-regulation [14]. Effectively, this polymer is known for its high thermal expansion, which disconnects the conducting path during the positive temperature coefficient (PTC) transition. The syndiotactic polystyrene is known for its chemical and thermal stability. Moreover, this polymer does not significantly alter the amplitude of the PTC effect and reduce the negative temperature coefficient (NTC) effect, which is a nondesirable feature because it corresponds to a decrease in electrical resistivity.

In this paper, the enhancement of the thermal conductivity brought on by adding aluminum oxide (Al_2O_3) or boron nitride (BN) is

analyzed through the electrothermal behavior of ohmic heating elements. In the first part, the thermophysical properties of three formulations (biphasic material with aluminum oxide or boron nitride and a reference one, called CPC1, without thermal conductive filler) were investigated. In the second part, experiments and numerical studies were realized to examine the electrical and thermal coupling phenomena on extruded tapes. The three characterized formulations were shaped like a tape for the purpose of heating experiments. The use of this geometry (tape measuring 10-cm long, 5-cm high, and 3-mm thick) facilitates the thermocouple implantation, in particular at the material core. On the other hand, this geometry makes the use of a 2-D model necessary because the temperature field in the material (through the thickness and the height) depends on the boundary conditions applied. Thus, FEMLAB® software was used to develop a 2-D finite element model to take thermal phenomena such as conduction, convection, and radiation, as well as electrical conduction, into account. To compare the simulated results with experiments, all thermophysical properties were used as input parameters in the modeling. Then, extrapolation to higher power density was performed with the validated model to show improvement in electrothermal performances by using thermal conductive fillers.

Materials and Techniques

Materials

The electrically conductive phase was high-density polyethylene provided by Atofina. The adjusted carbon black content was obtained by blending with a master batch filled with 23% volume/volume of CB (Vulcan XC 72-N472 from Cabot) made by Premix (PRE-ELEC TP 5813).

The thermal conductive phase was QUESTRA syndiotactic polystyrene from Dow Chemical. Thermal conductive fillers dispersed in the polystyrene syndiotactic (sPS) matrix: Al_2O_3 [15] and BN [16] were provided by Sigma–Aldrich and Métaux Céramiques Systèmes Engineering (MCSE) France, respectively. Some characteristics of the polymers and the fillers used are summarized in Tables 1 and 2.

Techniques

Each component was dried for 12 h under a vacuum at 90°C before blending. The blending process was carried out in three stages:

1) The electrically conducting phase was made by a HDPE blending with master batch HDPE-23% CB in a twin-screw extruder contrarotating Brabender at 20 or 30 rad · min^{-1}. The temperature profile from feed to die was 190/195/205°C.

2) Processing of the thermally conducting phase was obtained by mixing of sPS pellets with ceramic fillers in a single-screw extruder, Fairex. The mixing speed was 30 rad · min^{-1} and the temperature profile from feed to die was 275/277/280/280°C.

3) The elaboration of biphasic CPC was made by blending the electrical phase with the thermal phase in the twin-screw extruder contrarotating Brabender. Compounds were blended at 275/280/280°C with a mixing speed of 20 rad · min^{-1}. The die was a split of 5 × 50 mm to obtain tapes. No anisotropy is expected to be generated during this process.

The filler content was checked by thermogravimetric analysis using a Setaram TGA. The average weight of the samples was approximately 30 mg and the precision of measurements was estimated to be less than 0.5%.

Table 1 Main characteristics of polymers used

	HDPE	HDPE-CB	sPS
Glass transition temperature T_g, °C	−30	——	99
Melting temperature T_m, °C	133	133.6	275
Crystallization temperature $T_{c,n}$, °C	107	111.5	——
Crystallinity rate X, %	31	31	51
Density ρ, g · cm^{-3} at 25°C	0.95	0.93	1.05

The density measurements were carried out using a pycnometer at room temperature (27°C) in methanol. Given the sample size and filler shape, CPC are considered homogeneous at the macroscopic scale. Then, thermal expansion coefficient $\Delta L/L_0$ of the composite was measured by a dynamic mechanical analyzer (Model 2980 of Thermal Analysis (TA) Instruments) and used to determine the density variation as a function of temperature. The precision of this measurement was estimated to be better than 2% [12].

The calorimetric measurements were performed with a Mettler Toledo DSC 822. The calibration was done with indium and zinc. Aluminum pans with holes were used and the average sample mass was approximately 15 mg. All samples were first heated to 300°C for 5 min to get rid of thermal history. To prevent any sample degradation, the experiments were carried out under nitrogen flow.

Electrical resistivity as a function of temperature was measured by a four-point probe technique. Samples (2 × 10 × 80 mm) were placed in a programmable oven (from 20 to 180°C at 0.5°C · min^{-1}) [6].

The thermal diffusivity was determined by the flash method [17]. A short duration burst of energy delivered by a Nd/glass pulse laser of 10.6 μm wavelength with an energy pulse up to 8 J and a pulse duration of 0.4 ms, heats the surface of the material. The precision of these measurements was estimated to be close to 5%.

The thermal conductivity values calculated from the diffusivity were compared with the values obtained by direct measurement using the guarded hot plate technique at different temperatures: 30, 50, and 70°C [18]. The differences observed in the determination of k with the two techniques were less than 10%.

Thermophysical Properties

Electrically Conductive Phase

The electrical resistivity and the thermal conductivity of HDPE-CB as a function of carbon black volume fraction are plotted in Fig. 1. The electrical percolation threshold is the inflexion point of the curve describing the switch between an insulating and a conductive composite. The electrical resistivity exhibits an important resistivity drop of several decades between the percolation threshold and the maximum value studied, 23%, whereas the thermal conductivity is solely doubled with 23% of CB [k_{HDPE} being 0.34 W · m^{-1} · K^{-1} and k_c (HDPE-23% CB) is only 0.65 W · m^{-1} · K^{-1}]. More details and characteristics of the obtained conductive pathway through the material can be given and discussed in an electrical [6,11] and thermal [13] point of view either by the Kirkpatrick equation [19] or by thermal models [13].

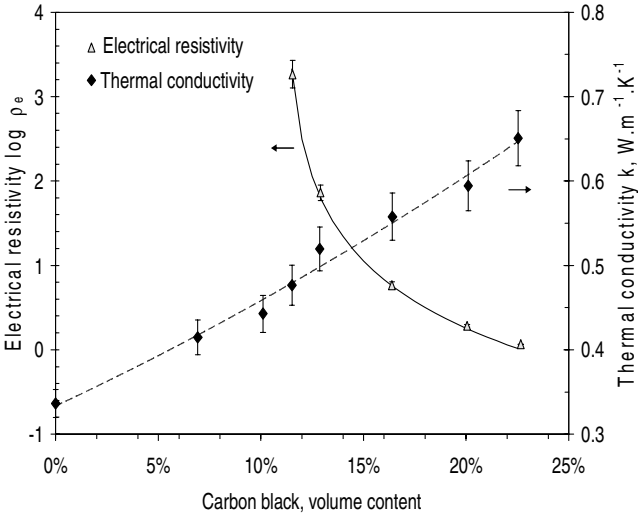

Fig. 1 Electrical resistivity and thermal conductivity of HDPE filled with CB.

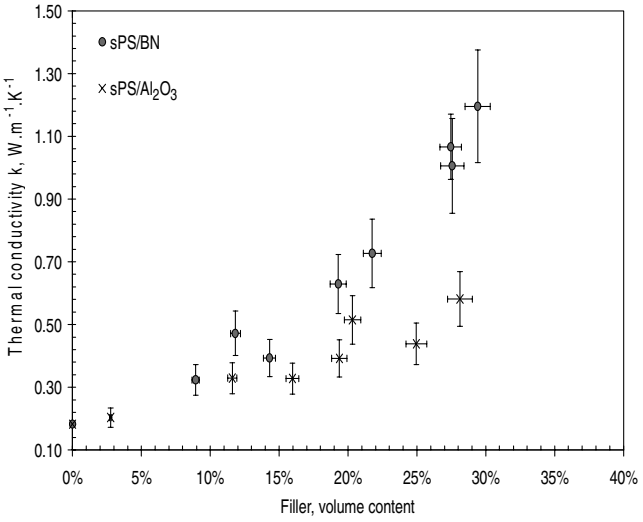

Fig. 2 Thermal conductivity of sPS filled with Al_2O_3 and BN.

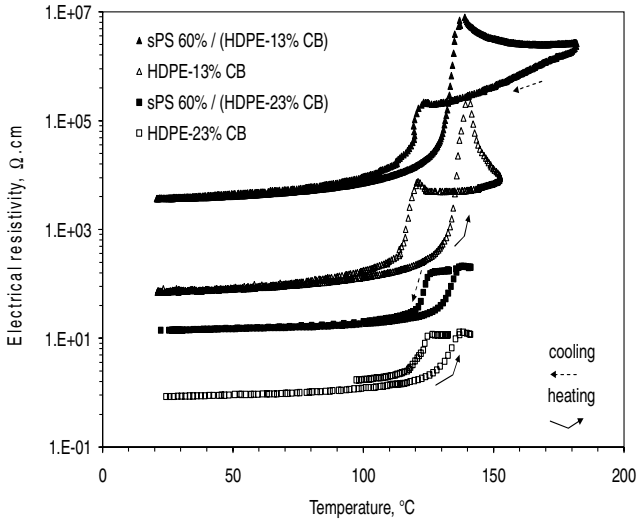

Fig. 3 Electrothermal behavior of HDPE-CB and sPS/HDPE-CB.

Insulating Electrical Phase with Thermally Conductive Fillers

Figure 2 presents the value of thermal conductivity as a function of the filler volume fraction at 300 K. It is remarkable that the composite filled with BN particles leads to a much higher conductivity rise than does the Al_2O_3 composite. The thermal conductivity of sPS/BN is noted to be twice that of the other composite at 30%. A complete thermal analysis of these composites is given in a previous work [13].

Biphasic Conductive Polymer Composites

Figure 3 shows the change in electrical resistivity of mono and biphasic CPC containing the same amount of CB in the electrically conductive phase during a heating/cooling cycle at $0.5°C \cdot min^{-1}$. The blend of the electrically conductive phase with 60% of sPS (corresponding to the phase inversion ratio in which both phases are cocontinuous) increases the electrical resistivity to almost two decades. On the other hand, the PTC effect remains unchanged when adding sPS and increases with the decrease in CB content, which is coherent because CB particles are more easily disconnected when the sample is undergoing thermal dilatation during heating. The heating occurs over the melting temperature of the electrically conductive phase (HDPE), leading to a NTC phenomenon due to an increase in molecular mobility [14]. This undesirable phenomenon is slightly reduced by the sPS presence and, hence, a decrease in the self-destruction capability of the system when overheating. The hysteresis during cooling is explained by the temperature difference between melting and crystallization.

In this study, three formulations are tested (see Table 3). In all formulations, the amount of carbon black is arbitrarily set to 23% in HDPE. The electrically conductive phase is then blended with the so-called thermally conductive phase, which is around 60% in volume to insure cocontinuous morphology.

Figure 4 presents the electrical resistivity during a thermal cycle from room temperature to 180°C at 0.5°C/ min. The plots correspond to the second cycle. The first cycle is used to get rid of the thermal history. Adding thermal conductive fillers does, however, have a slight impact on the electrical resistivity, as can be seen in Fig. 4. The difference in ratio between the sPS and the HDPE phases may partially explain it at room temperature. At higher temperatures, we can see that the ceramic particles also influence the crystallization of the HDPE phase (see Fig. 5) and, hence, a shift of CPC2 and CPC3 cooling to a higher temperature.

Figure 5 shows that the HDPE crystallization temperature is shifted to a higher temperature as a function of the nucleating effect of thermal conductive fillers (+5°C with Al_2O_3 and +10°C with BN). This means that the ceramics fillers are partially coated by the HDPE phase. On the other hand, the melting temperature is similar for all biphasic CPC.

Figure 6 shows the change in thermal expansion of the materials tested. CPC1 [sPS 53%/(HDPE-23% CB)] presents a sharp increase in thermal expansion from 100°C (and, consequently, a decrease in the density with temperature). This is mainly due to the melting of

Table 2 Filler properties

Filler	Aluminum oxide	Boron nitride	Vulcan XC72
Chemical formula	Al_2O_3	BN	CB
Density ρ,g $\cdot$ cm^{-3}[a]	4.00	2.30	1.8
Melting temperature T_m, °C[a]	2054	3027	——
Thermal conductivity k_f, W $\cdot$ m^{-1} $\cdot$ K^{-1}, at 300 K[a]	36	125	6–175 [24]
Specific heat C_p, J $\cdot$ kg^{-1} $\cdot$ K^{-1}, at 300 K[a]	776	730	——
Electrical resistivity ρ_e, $\Omega \cdot$ cm, at 300 K[a]	10^{14}	2×10^{14}	——
Particle diameter,μm	11	8	30×10^{-3}
Shape factor [13]	5.6 [13]	79 [13]	——

[a]From producer.

Table 3 Formulations of biphasic CPC

CPC	Thermal conductive phase	Electrical conductive phase	ϕ% of thermal conductive phase
CPC1	sPS	HDPE-23% CB	55%
CPC2	sPS-28% Al_2O_3	HDPE-23% CB	60%
CPC3	sPS-32% BN	HDPE-23% CB	63%

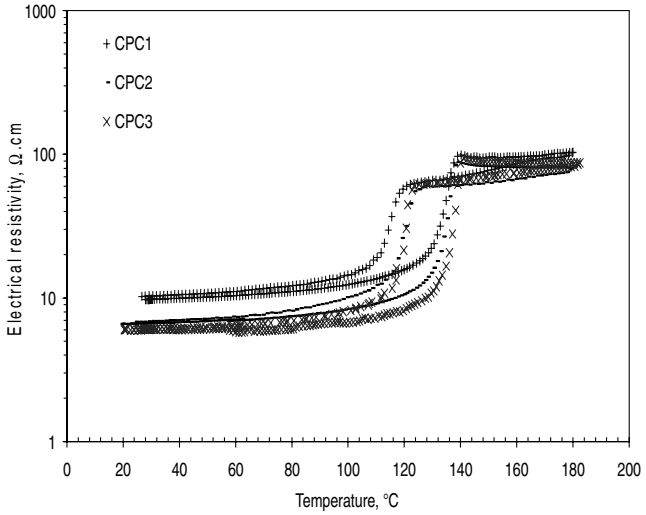

Fig. 4 Electrical resistivity of tested biphasic CPC.

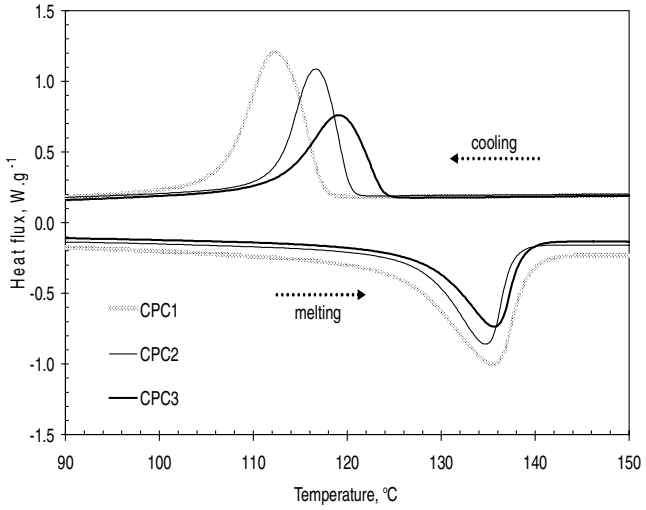

Fig. 5 Heat flux of biphasic CPC (HDPE melting and crystallization) from 90 to 150°C.

HDPE crystals. The linear thermal coefficient undergoes a change of slope from 90 to 160 $\mu m \cdot m^{-1} \cdot K^{-1}$ at this temperature. The change of the slope given by the sPS T_g (glass transition) is less significant than that of HDPE melting. When the biphasic contains thermally conductive fillers, the change of slope is less significant: 20% instead of the previous 78%. At 27°C, the density of each biphasic CPC is given in Table 4.

Table 4 Density of composites at 27°C

Material	Density, $kg \cdot m^{-3}$, at 27°C	Linear thermal coefficient, $\mu m \cdot m^{-1} \cdot K^{-1}$
CPC1	1086 ± 13	92, −2%
CPC2	1578 ± 18	73, 0%
CPC3	1339 ± 12	49, −8%

The change in specific heat with temperature is presented in Fig. 7. The glass transition of pristine sPS is clearly visible (curve 3), whereas in the CPC containing a HDPE phase, the glass transition of sPS vanishes due to the high melting enthalpy of HDPE crystals (ΔH_m of 95 $J \cdot g^{-1}$ against 27.2 $J \cdot g^{-1}$ only for sPS), although the crystalline rate of HDPE is 31% and 51% for sPS.

The values of thermal conductivity with temperature were evaluated from the measurement of diffusivity, density, and specific heat [Eq. (1)]:

$$k = \alpha \rho C_p \tag{1}$$

To check the results, the thermal conductivity measured at 50°C by a guarded hot plate is punctually compared (Table 5). The variation in the thermal conductivity as a function of temperature is presented in Fig. 8. As for the previous properties, ρ and c_p, the evolution of the thermal conductivity is restricted by the two constituent phases sPS and HDPE-23% CB.

The biphasic CPC filled with boron nitride (CPC3) presents a stable progression unlike the other biphasic CPC that are more like the HDPE-23% CB. This can be explained by the very low thermal expansion of CPC filled with BN (Fig. 6). As shown in Table 5, the thermal conductivities of the biphasic CPC filled with thermal conductive fillers are both lower than that of the constituent phase. This odd drop in thermal conductivity can partially be explained by a coating of the HDPE phase over the thermal conductive fillers, which leads to a decrease in the particles' interconnectivity [13].

At this stage of the study, we have shown that it is possible to process new biphasic CPC. The study of their thermophysical properties put into evidence the followings points:

1) It is possible to adjust the electrical resistivity apart from the thermal conductivity by changing the suitable filler content.

2) Adding thermally conductive fillers does not increase the electrical resistivity or even alter the PTC effect. In fact, it was shown that this addition slightly improves the electrical conductivity.

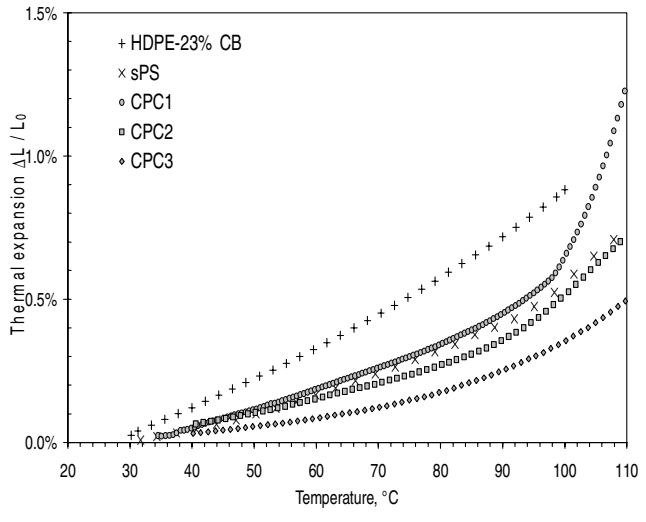

Fig. 6 Thermal expansion of composites from 27 to 110°C.

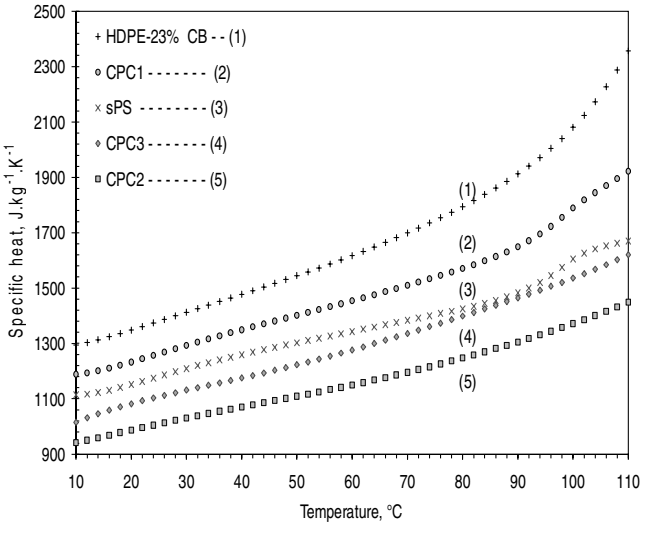

Fig. 7 Specific heat of composites from 10 to 110°C.

Table 5 Experimental thermal conductivity of CPC at 50°C

Material	CPC1	CPC2	CPC3
Thermal conductive phase	0.18	0.65	0.74
Electrical conductive phase	0.63	0.63	0.63
CPC [from Eq. (1)]	0.33	0.55	0.60
CPC (guarded hot plate)	0.31	0.57	0.59

3) A nucleating effect was measured not only on the sPS phase but also on the HDPE phase. This demonstrates the presence of thermally conductive filler dispersed in the HDPE phase.

4) A decrease in the thermal conductivity compared with that in the constituent phases was also noticed. This is explained by the presence of thermally conductive fillers dispersed in the HDPE phase, which decreases the interconnectivity of particles.

The knowledge of the thermophysical properties with temperature is exploited in the next part of this paper to simulate the electrothermal behavior of extruded tapes used as heating elements.

Study of Electrothermal Behavior of Conductive Polymer Composites Tapes

The electrothermal behavior of CPC extruded tapes subjected to a potential difference is studied. The electrical current crossing does lead to an overheating by the joule effect. However, the voltage is slow enough to allow heat dissipation by free convection. Experiments and numerical studies were realized to examine the electrical and thermal coupling phenomena. These studies give a better understanding of the influence of thermal and electrical conductivities on CPC behavior used as a heating element.

The tested configuration is presented in Fig. 9. The CPC is subjected to direct current by two electrodes set at the ends of the sample tape (Fig. 9). The power generated by the joule effect in the CPC is dissipated in surroundings by free convection and long infrared radiation. The tapes are laid vertically to get symmetry of heat exchanges. The size of elements is about 10-cm long, 5-cm high, and 3-mm thick.

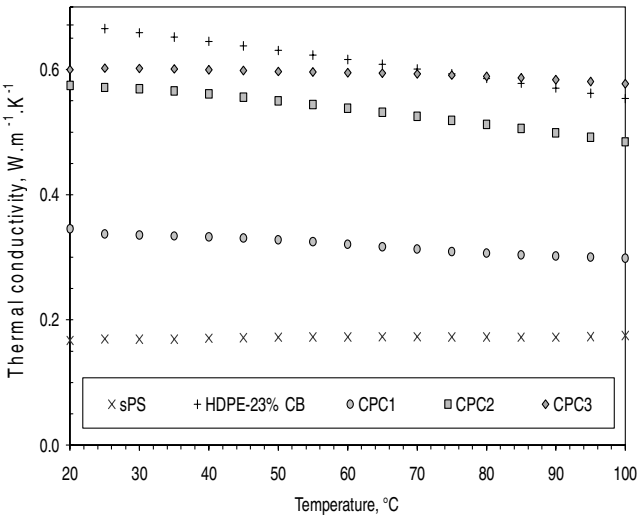

Fig. 8 Thermal conductivity of composites from 20 to 100°C.

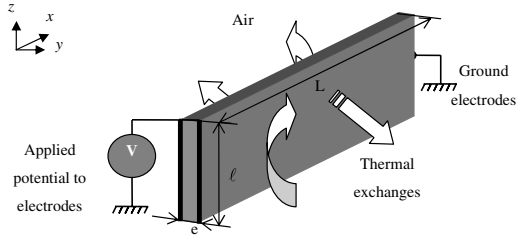

Fig. 9 Specification of the system.

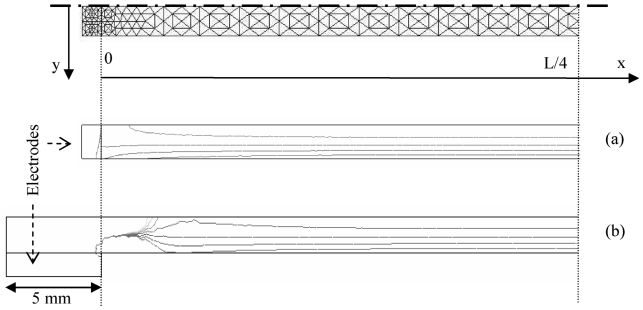

Fig. 10 Current density lines for different settings of electrodes: a) applied to the ends, and b) stacked.

Modeling

To model the electrothermal behavior of the CPC tape, the geometry and the boundary conditions are required to develop a 3-D model, which takes the electrical and thermal conduction in the CPC and the electrical and thermal boundary conditions into account. To reduce the complexity of the problem (2-D model), we have initially checked the uniformity of the current density field along the tape length. Indeed, the electrode settings have an influence on the heat source generated (in particular, the current density). To evaluate this influence, simulations have been carried out on a lengthwise slice of tape with different copper electrode settings (Fig. 10).

A 2-D model is then developed to evaluate the thermal field in the tape. The temperature field in the material is a function of the x and y axes. It depends on the boundary conditions applied. A correlation giving the convective heat coefficient for a vertical plane surface whose temperature evolves according to the height does not exist in the scientific literature. In this study, the temperature or the flux density along the z axis is not constant. It is necessary, then, to develop a model of the flow around the band to evaluate the field of temperature and the convective heat exchange between the band and the fluid. The heat exchanges are supposed two-dimensional (y, z) and, due to symmetry, only a half-thickness is modeled (Fig. 11).

A mathematical model representing the electrothermal behavior of the studied system has been developed with FEMLAB. This software uses the finite element method [20]. The domain was discretized in triangular elements and a quadratic interpolation was used for each output. For each model, the mesh was tested to obtain the same solution with a minimum of elements. Thus, the grid contained about 100 elements for the study of electrical boundary conditions and up to several thousand elements for the study of thermal boundary conditions.

Electrical and Thermal Conduction Equations in Conductive Polymer Composites

Electrical conduction in a material supposed homogeneous and isotropic is governed by the Laplace equation, in which σ is the

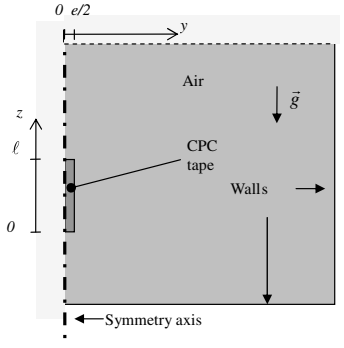

Fig. 11 Complete scheme of the tape section with air flowing out.

electrical conductivity [21]:

$$-\nabla \cdot (\sigma \nabla V) = 0 \tag{2}$$

The phenomena of thermal conduction are given by the heat equation

$$\rho C_p \frac{\partial T}{\partial t} = \nabla \cdot (k \nabla T) + \sigma E^2 \tag{3}$$

The electrothermal coupling takes place in the term $\langle\langle \sigma E^2 \rangle\rangle$, which represents the internal heat source generated by the joule effect.

The variation of the thermophysical properties of CPC (σ, k, ρ, C_p) as a function of temperature was integrated into the polynomial equations.

Thermal Equations in Fluid

In this study, the flow around the CPC remains laminar and is governed by the continuity, Navier–Stokes, and energy equations. The fluid is supposed incompressible and Newtonian.

Continuity equation:

$$\nabla \cdot \mathbf{U} = 0 \tag{4}$$

Navier–Stokes equations:

$$\rho(\mathbf{U} \cdot \nabla)\mathbf{U} - \eta \nabla^2 \mathbf{U} + \nabla p = \mathbf{F} \quad \text{with} \quad F_z = -\rho g \beta (T - T_{\text{air}})$$
$$F_y = 0 \tag{5}$$

Energy equation:

$$\nabla \cdot (k \nabla T - \rho C_p T \mathbf{U}) = 0 \tag{6}$$

In these equations, $\mathbf{U}$ represents the air velocity field ($\text{m} \cdot \text{s}^{-1}$), ρ is the density, η is the dynamic viscosity (Pa · s), p is the pressure (Pa), g is the gravitational acceleration ($\text{m} \cdot \text{s}^{-2}$), and β is the coefficient of thermal expansion (K^{-1}). The air thermophysical properties are assumed as polynomial functions of temperature.

Interface and Boundary Conditions

At the interface CPC fluid, the radiative flux density φ is taken into account in the model by Necati Özisik, M.[22]:

$$\varphi = \varepsilon \sigma_s \left(T_{\text{wall}}^4 - T_s^4 \right) \tag{7}$$

where σ_s is the Stefan–Boltzmann constant $\text{W} \cdot \text{m}^{-2} \cdot \text{K}^{-4}$, ε is the emissivity of the CPC, T_s is the surface temperature of the CPC, and T_{wall} is the experimental wall temperature.

At the walls, the velocity is set to zero and the temperature is imposed to the experimental wall temperature. On the vertical symmetric axis, all the perpendicular gradients (temperature, velocity, and pressure) are null.

Influence of Electrodes

No matter what the setting or size of the electrodes is, the interelectrode distance is 100 mm and the electrical contact between the electrode and the CPC is supposed perfect. Moreover, along the tape surface a constant thermal exchange coefficient of 20 $\text{W} \cdot \text{m}^{-2} \cdot \text{K}^{-1}$ is applied.

Because of symmetrical reasons, a half-thickness of the band is modeled. The mesh is given in Fig. 10, in which the electrode is 5-mm long and 1-mm thick. The results obtained are presented for the two different settings tested. Each line represents an isocurrent level. The isocurrent range is the same in each setting. We can see that the current density is relatively homogeneous along the x axis after 5 mm away from the electrode. Then, a vertical slice (y, z) at the middle length can be used for the study of thermal boundary conditions.

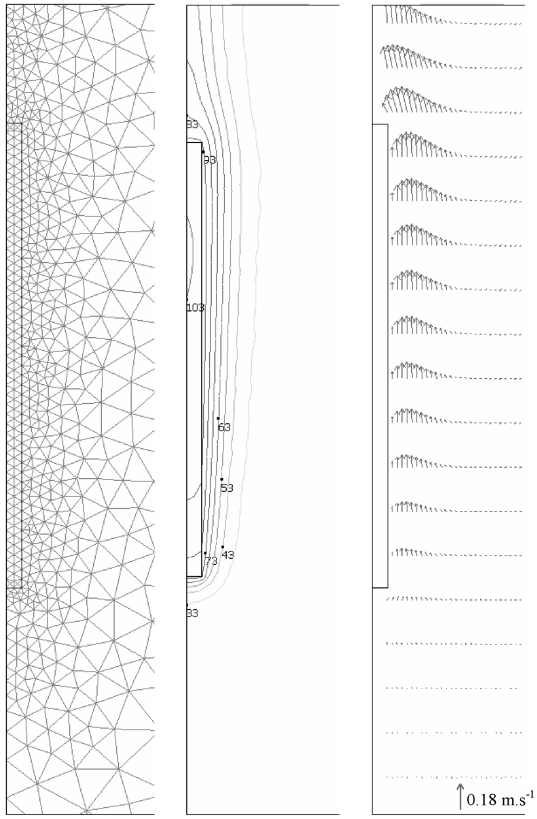

a) b) c)

Fig. 12 CPC2/2-D model: a) mesh, b) contour of temperature, and c) velocity vectors in stationary state for $P = 764$ kW · m^{-3}.

Two-Dimensional Model

The heat exchanges are supposed two-dimensional (y, z), and due to symmetry, only a half-thickness is modeled (Fig. 11). The domain is discretized in 6000 triangular elements. A fine mesh has been used to correctly model the thermal boundary layer that develops itself at the tape surface. Figure 12 presents an example of mesh, a contour map of temperature, and the velocity vectors. We can note that the velocity and the temperature (and so the convective heat coefficient) are very different according to the z axis.

Experiments

The experimental approach developed in this work is based on the previous studies carried out with CPC tapes filled with carbon black and carbon fibers [6,12,23]. This study is focused on a vertical section placed along the half-length tape.

The tests are carried out with extruded tape of 10 cm in length, which is sufficient to neglect the influence of the electrodes (see Fig. 10). The section size was imposed by the extruder die, which gives the tape about a 50-mm width and a 3-mm thickness. The technique chosen for the electrode settings is the same for all tapes. The copper electrodes were warmed before being pressed to the tape ends to reduce electrical contact resistances.

The temperature response was provided by K-type thermocouples set at the center and at the surface of the tape (Fig. 13). These thermocouples were embedded at half-height (Fig. 13). On each side of the tape, thermocouples measured the surrounding air temperature. The temperature, voltage, and intensity were read as a function of time by an acquisition system. The experimental uncertainty was essentially coming from the measurement of temperature (±1.5°C), voltage (±0.5 V), and intensity (±2 mA), and the location of thermocouples in situ (±50 μm in depth and ±500 μm in height).

Before the experiment, tapes were heated at 150°C for 1 h in an oven. The oven temperature was then slowly decreased below the CPC crystallization temperature to control and homogenize the

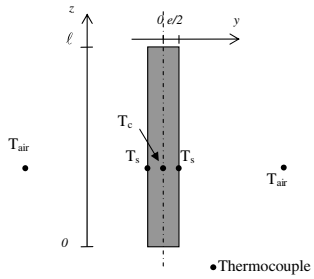

Fig. 13 Tape instrumentation.

crystalline structure. The exact sizes and the electrical resistances of the three tapes are summarized in Table 6.

Results and Discussion

Experimental Tests

The tapes are subjected to regular voltage steps. The protocol is common for each material: three increasing and then decreasing steps of 10 V between 0 and 30 V. The time step, from 10 to 30 min, is sufficiently long to allow steady state to occur. The maximum potential difference applied was chosen to get a maximum temperature of 110°C using the tape with the lowest electrical resistance (CPC2), corresponding to an acceptable temperature for the long run.

Figure 14 presents the temperature and intensity responses for CPC1. The surface and air temperature plots correspond to the means measurement performed on each tape side. The self-regulation phenomenon is put into evidence by intensity peaks occurring at the beginning of each voltage step. In steady state, at 30 V corresponding to an exchange heat flux of about 0.8 $kW \cdot m^{-2}$, the measured temperature reaches 93°C at the center and 91°C at the surface, giving a difference of 2°C over 1.46 mm of thickness.

Figure 15 emphasizes the change of the experimental temperature gradient as a function of the heat flux density. The temperature gradient is measured at half-height and corresponds to the temperature difference between the center and the surface. The experimental errors occurring are numerous: thermocouple position; smoothness, evenness, and straightness of the tape surface; and tape and measurement uncertainty. Despite all these experimental errors, the results are quite linear and coherent. The slopes of the straight lines in Fig. 15 are inversely proportional to the CPC thermal conductivity (the tape with the highest thermal conductivity, CPC3, is thus the one with the lowest slope).

The evolution of the electrical resistivity of the tapes according to the temperature can also be calculated from the measurements carried out throughout these experiments (Fig. 16). At 30°C, the CPC filled with boron nitride is equivalent to CPC1 (9.3 ± 0.9 $S \cdot m^{-1}$), whereas the CPC with aluminum oxide has a slightly higher electrical conductivity: 10.3 ± 0.9 $S \cdot m^{-1}$. This change and level of electrical conductivity is coherent with previous measurements carried out on smaller samples (Fig. 4).

Experimental and Numerical Comparison

First, we compare, in steady state, the numerical and experimental results for the CPC2 material. In this case, a part of the tape temperature exceeds 100°C.

Figure 17 gives the vertical temperature profiles at the center and at the tape surface obtained from the 2-D model for a voltage of 30 V. An important variation of the temperature according to the z axis can

Table 6 Size and electrical resistance of tapes

Tape	Length L, mm	Height l, mm	Thickness e, mm	Electrical resistance at 30°C, Ω
CPC1	101	40	2.9	94
CPC2	100	47	3.2	64
CPC3	102	47	2.5	82

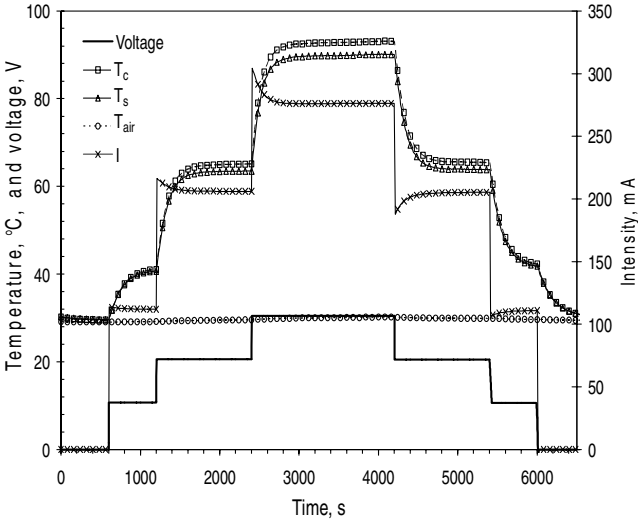

Fig. 14 Experimental test: intensity and temperature responses of CPC1.

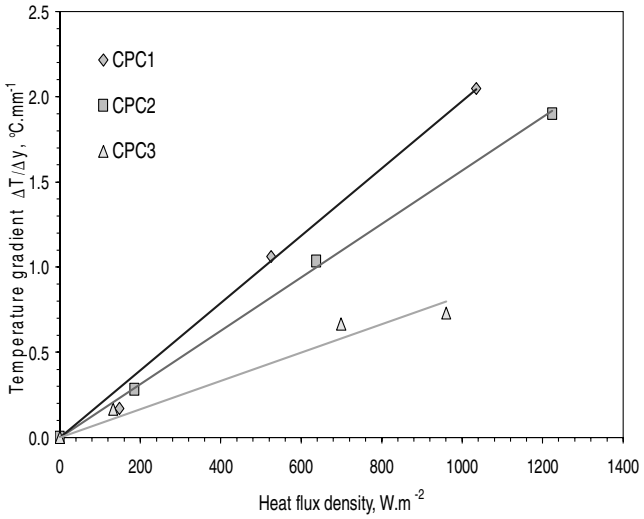

Fig. 15 Temperature gradient as a function of heat flux density (different voltage levels: 10, 20, 30 V).

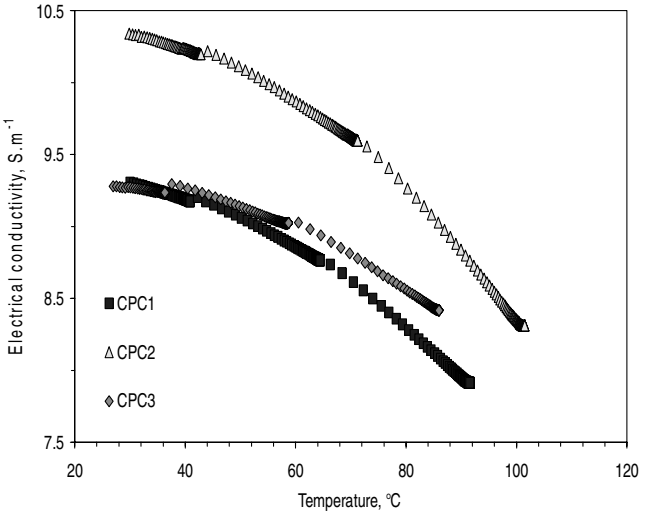

Fig. 16 Electrical conductivity of the materials used as a function of temperature.

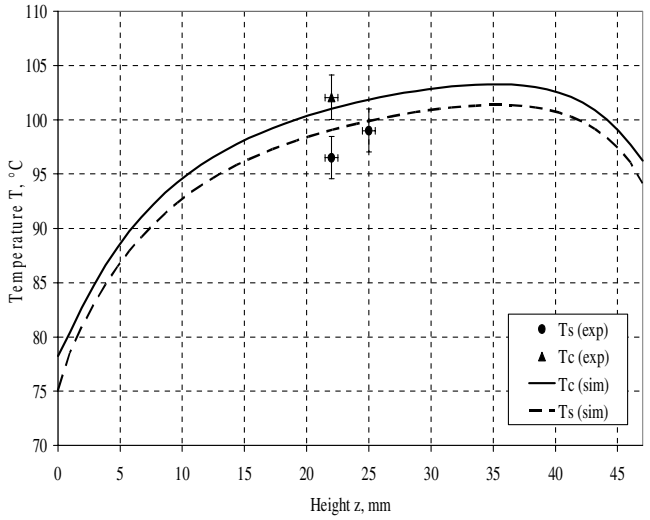

Fig. 17 CPC2/2-D model: simulated and experimental temperatures along the height at the center and at the tape surface at 30 V.

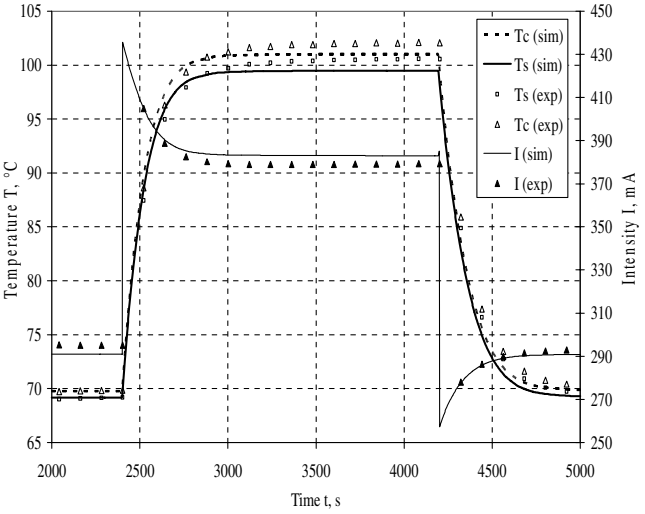

Fig. 19 CPC2: experimental data and simulation comparison during the 20–30 V step ($z = 23.5$ mm).

be noted. In this figure, the experimental temperatures are also plotted by taking their location into account. The comparison between experimental and simulated results shows an acceptable gap concerning the uncertainties of the material properties and the experiments.

To complete this analysis, the simulated temperature and the current density profiles along the y axis (thickness) are plotted in Fig. 18. To confirm the simulations, the current is calculated from the current density by the expression

$$I = 2\int_S J\,\mathrm{d}S = 2\int_S \frac{\sigma(T)V}{L}\,\mathrm{d}S \tag{8}$$

and compared with the measurements. In this case, the simulated result (383 mA) is very close to the measured intensity 379 mA.

Figure 19 presents the experimental and simulated responses obtained during the 20–30 V step. The simulated temperatures correspond to values obtained at $z = 23.5$ mm. The measurements and the simulated results (temperatures and current) correlate well during both heating and cooling. The study of sensitivity shows that a change of 5% of the electrical conductivity induces a modification of about 4% of the current density profile and the temperature. Regarding the thermal conductivity, we obtain a small impact inside the material and almost none at the surface. The same study performed on the other two materials (CPC1 and CPC3) leads to comparable observations.

Simulation of Flux Density Influence

The tests carried out in free convection conditions do not permit one to study the impact of higher flux density (>1 kW $\cdot$ m^{-2}). Thus, a stationary 1-D model has been used [$T(y)$]. In the simulations, the global heat exchange coefficient (convection and radiation) is constant during calculation and is gradually increased when the internal inputs increase to keep the tape center below 100°C, an acceptable temperature for these polymers. This extrapolation is represented in Fig. 20, in which the difference of temperature between the center and the surface tape (ΔT) is plotted as a function of the dissipated heat flux. These results are given for each material and for two thicknesses (2 and 3 mm). These plots are linear because the thermal conductivity of the materials is constant in the temperature range involved during these simulations and their thermal expansions (relatively low) are not taken into account either.

This figure highlights an important issue of this study. For instance, for a power density of 20 kW $\cdot$ m^{-2}, the difference of temperature for the CPC1 tape of 3 mm ($k = 0.33$ W $\cdot$ m^{-1} $\cdot$ K^{-1}) would be about 46°C. In these conditions, high mechanical stresses are involved, which could, in the long run, damage the system. To decrease this destructive temperature difference, this graph shows

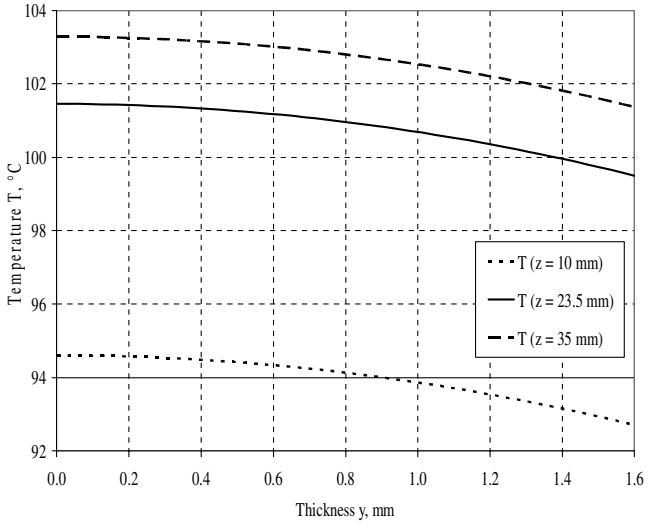

a)

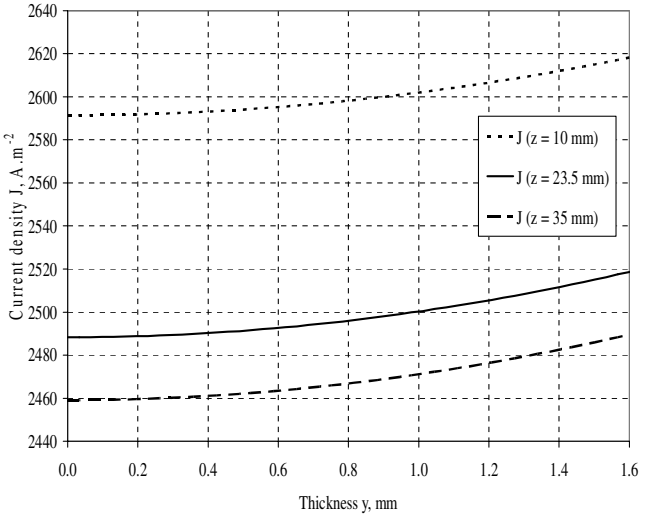

b)

Fig. 18 CPC2/2-D model: a) temperature, and b) current density profiles through the thickness at 30 V.

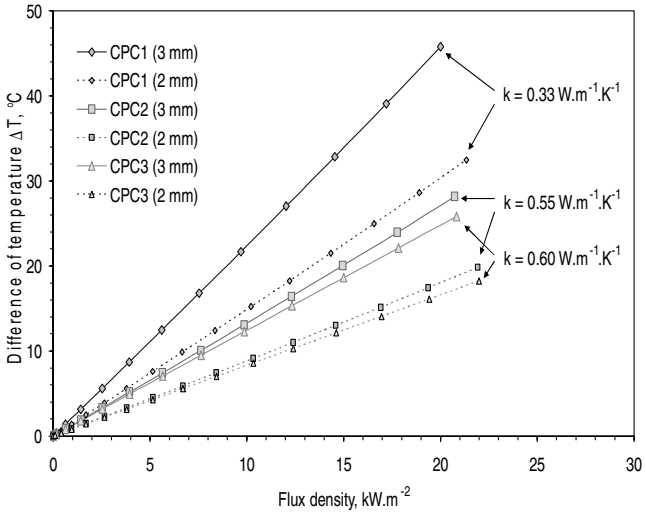

Fig. 20 Thermal difference in the material as a function of the heat flux density for two thicknesses (2 and 3 mm).

that two solutions are conceivable: increase the thermal conductivity and/or reduce the thickness of the material.

Conclusions

In this paper, biphasic conductive polymer composites for heating applications have been investigated. Their polymer matrices, which are good thermal insulators, are usually a major drawback for reaching high power density levels when used as heating elements. The improvement of the thermal conductivity was thus our first concern in this study.

The first part of this paper dealt with the biphasic material study containing polystyrene syndiotactic and high-density polyethylene. We showed that it is possible to adjust the electrical resistivity apart from the thermal conductivity to obtain new CPC, with good electrical and thermal conductivity, in the condition of optimizing a formulation according to the applications concerned. The electrical phase was obtained by carbon black filled in HDPE. In this system, the electrical percolation threshold was 11% v/v. For the thermal conductive phase (with sPS), these studies demonstrated that the thermal conductivity is strongly increased with a filler amount of up to 30% v/v of microparticles of boron nitride or aluminum oxide. Three polymer composites were created and their material properties analyzed. The addition of the ceramic powder (20%) to the polymer composites enhanced the thermal conductivity of the CPC (×2) without significantly modifying the electrical conductivity of the composites.

Additionally, computational models and experiments were used to examine and characterize the electrical and thermal behavior of these CPC tapes. The experiments were carried out in free convection in air with power density exchanged lower than 1 $kW \cdot m^{-2}$. We have shown that the simulated thermal and electrical responses correlated well among experiments. This allowed their behavior to be predicted for a higher level of power density, used as a heating element system. The results show the importance of adding thermally conductive fillers to the tape to decrease the thermal gradients inside the tapes and consequently reduce thermally induced mechanical stresses. Therefore, when a CPC device needs high power dissipation, adding a thermally conductive filler such as boron nitride is interesting.

References

[1] Huang, J-C., "Carbon Black Filled Conducting Polymers and Polymer Blends," *Advances in Polymer Technology (USA)*, Vol. 21, No. 4, 2002, pp. 299–313. doi:10.1002/adv.10025

[2] Xue, Q., "The Influence of Particle Shape and Size on Electric Conductivity of Metal-Polymer Composites," *European Polymer Journal*, Vol. 40, No. 2, 2004, pp. 323–327. doi:10.1016/j.eurpolymj.2003.10.011

[3] Chung, D. D. L., "Self-Heating Structural Materials," *Smart Materials and Structures*, Vol. 13, No. 3, 2004, pp. 562–565.doi:10.1088/0964-1726/13/3/015.

[4] Wang, X., and Chung, D. D. L., "Short Carbon Fiber Reinforced Epoxy Coating as a Piezoresistive Strain Sensor for Cement Mortar," *Sensors and Actuators. A, Physical*, Vol. 71, No. 3, 1998, pp. 208–212. doi:10.1016/S0924-4247(98)00187-3

[5] Bartlett, P. N., Archer, P. B. M., and Ling-Chung, S. K., "Conducting Polymer Gas Sensors. Part 1: Fabrication and Characterization," *Sensors Actuators*, Vol. 19, No. 2, 1989, pp. 125–140.

[6] Glouannec, P., Chauvelon, P., Feller, J.-F., Noel, H., and Ploteau, J.-P., "Current Passage Tubes in Conductive Polymer Composite for Fluid Heating," *Energy Conversion and Management*,Vol. 49, No. 4, April 2008, pp. 493–505.doi:10.1016/j.enconman.2007.08.013.

[7] El-Tantawy, F., Kamada, K., and Ohnabe, H., "In Situ Network Structure, Electrical and Thermal Properties of Conductive Epoxy Resin-Carbon Black Composites for Electrical Heater Applications," *Materials Letters*, Vol. 56, Nos. 1–2, 2002, pp. 112–126. doi:10.1016/S0167-577X(02)00401-9

[8] Chiu, H.-T., and Chiu, W.-M., "Influence of Mechanical Properties in Carbon Black CB Filled Isotactic Polypropylene iPP and Propylene-Ethylene Block Copolymer," *Journal of Applied Polymer Science*, Vol. 61, No. 4, 1996, pp. 607–612. doi:10.1002/(SICI)1097-4628(19960725)61:4<607::AID-APP4>3.0.-CO;2-P

[9] Abdel-Bary, E. M., Amin, M., and Hassan, H. H., "Factors Affecting Electrical Conductivity of Carbon Black-Loaded Rubber. I. Effect of Milling Conditions and Thermal-Oxidative Aging on Electrical Conductivity of Half Carbon Black-Loaded Styrene-Butadiene Rubber," *Journal of Polymer Science: Polymer Chemistry Edition*, Vol. 15, No. 1, 1977, pp. 197–201. doi:10.1002/pol.1977.170150118

[10] Zee, F., and Judy, J. W., "Micromachined Polymer-Based Chemical Gas Sensor Array," *Sensors and Actuators. B, Chemical*, Vol. 72, No. 2, 2001, pp. 120–128. doi:10.1016/S0925-4005(00)00638-9

[11] Foulger, S. H., "Reduced Percolation Thresholds of Immiscible Conductive Blends," *Journal of Polymer Science Part B: Polymer Physics*, Vol. 37, No. 15, 1999, pp. 1899–1910. doi:10.1002/(SICI)1099-0488(19990801)37:15<1899::AID-POLB14>3.0.CO;2-0

[12] Droval, G., Glouannec, P., Feller, J.-F., and Salagnac, P., "Simulation of Electrical and Thermal Behavior of Conductive Polymer Composites Heating Elements," *Journal of Thermophysics and Heat Transfer*, Vol. 19, No. 3, 2005, pp. 375–381. doi:10.2514/1.12718

[13] Droval, G., Feller, J.-F., Salagnac, P., and Glouannec, P., "Thermal Conductivity Enhancement of Electrically Insulating Syndiotactic Poly (styrene) Matrix for Diphasic Conductive Polymer Composites," *Polymers for Advanced Technologies*, Vol. 17, Nos. 9–10, 2006, pp. 732–745. doi:10.1002/pat.777

[14] Feller, J.-F., "Conductive Polymer Composites: Influence of Extrusion Conditions on Positive Temperature Coefficient Effect of Polybutylene Terephthalate/Polyolefin-Carbon Black Blends," *Journal of Applied Polymer Science*, Vol. 91, No. 4, 2004, pp. 2151–2157. doi:10.1002/app.13337

[15] Agari, Y., Tanaka, M., Nagai, S., and Uno, T., "Thermal Conductivity of a Polymer Composite Filled with Mixtures of Particles," *Journal of Applied Polymer Science*, Vol. 34, No. 4, 1987, pp. 1429–1437. doi:10.1002/app.1987.070340408

[16] Ishida, H., and Rimdusit, S., "Very High Thermal Conductivity Obtained by Boron Nitride-Filled Polybenzoxazine," *Thermochimica Acta*, Vol. 320, Nos. 1–2, 1998, pp. 177–186. doi:10.1016/S0040-6031(98)00463-8

[17] Parker, W. J., Jenkins, R. J., Buttler, G. P., and Albott, G. L., "Flash Method of Determining Thermal Diffusivity Heat Capacity and Thermal Conductivity," *Journal of Applied Physics*, Vol. 32, No. 9, 1961, pp. 1679–1684. doi:10.1063/1.1728417

[18] Salmon, D., "Thermal Conductivity of Insulations Using Guarded Hot Plates, Including Recent Developments and Sources of Reference Materials," *Measurement Science and Technology*, Vol. 12, No. 12, 2001, pp. R89–R98. doi:10.1088/0957-0233/12/12/201

[19] Kirkpatrick, S., "Percolation and Conduction," *Reviews of Modern Physics*, Vol. 45, No. 4, 1973, pp. 574–588. doi:10.1103/RevModPhys.45.574

[20] Zienkiewicz, O. C., and Taylor, R. L., *Finite Element Method*, 5th ed., Butterworth–Heinemann, Boston, 2000.
[21] Metaxas, A. C., *Foundations of Electroheat*, Wiley, Chichester, England, U.K., 1996.
[22] Necati Özisik, M., *Heat Transfer*, A Basic Approach, McGraw–Hill, New York, 1985.
[23] Feller, J.-F., Glouannec, P., Salagnac, P., Droval, G., and Chauvelon, P., "Simulation of Electrical and Thermal Behavior of Polypropylene/Carbon Filler Conductive Polymer Composites," *Macromolecular Symposia*, Vol. 222, No. 1, 2005, pp. 187–194. doi:10.1002/masy.200550424
[24] Wolff, S., and Wang, M. J., *Carbon Black Science & Technology*, 2nd ed., Vol. 9, Marcel Dekker, New York, 1993, pp. 289–355.